DELPHI Collaboration DELPHI 2000–014 CONF 335
March 8, 2000

Search for Single Production of Leptoquarks in e^+e^- annihilations at $\sqrt{s}$ =192-202 GeV

Preliminary

S. Andringa[1], P. Gonçalves[1], A. Onofre[1], R. Paiva[1], L. Peralta[1], M. Pimenta[1] and B. Tomé[1]

Abstract

A search for events with one jet and at most one isolated lepton (charged or neutral) has been performed using data taken at LEPII by the DELPHI detector. The data analysed was accumulated at center-of-mass energies ranging from 192 GeV to 202 GeV and corresponds to a total integrated luminosity of 227 pb^{-1}. Production of single scalar and vector leptoquarks was searched for. Limits at 95% confidence level were derived within two different frameworks (direct processes and resolved photon processes), on the masses and couplings of the leptoquark states.

[1] LIP-IST-FCUL, Av. Elias Garcia, 14, 1, P-1000 Lisboa, Portugal

1 Introduction

In e^+e^- colliders such as LEP it is possible to search for New Physics in topologies where the expected Standard Model (SM) contributions are low or negligible. Events where all or most particles are grouped in one direction in space, in a mono-jet like topology, with one isolated lepton (charged or neutral), are a good example of such processes. SM extensions related to leptoquark models can have such a signature. The aim of the analysis reported in this paper is to perform a topological search for this channel [1].

Data were collected with the DELPHI detector at $\sqrt{s}$ ranging from 192 GeV to 202 GeV and correspond to a total integrated luminosity of 227 pb^{-1}.

Leptoquarks are coloured spin 0 or spin 1 particles which carry both baryon and lepton quantum numbers. These particles are predicted by a variety of extensions of the SM, from Grand Unified Theories [2] to Technicolor [3] and composite models [4]. They have electric charges of $\pm 5/3$, $\pm 4/3$, $\pm 2/3$ and $\pm 1/3$, and decay into a lepton and quark pair through the charged decay mode ($L_q \to l^{\pm} q$) and/or the neutral decay mode ($L_q \to \nu q$). Two hypotheses are considered in this paper, one where only the charged decay mode is possible (charged branching ratio $\beta = 1.0$), and one where both charged and neutral decay modes are equally probable ($\beta = 0.5$). Leptoquarks can be pair or singly produced at e^+e^- colliders, but only the single leptoquark search is considered in this analysis. The decays of singly produced high mass leptoquarks are characterised by a high transverse momentum jet recoiling against a lepton. In the neutral decay mode only the jet is detected.

Below the TeV mass range and for couplings of the order of the electromagnetic coupling, the allowed leptoquarks should not couple to diquarks in order to prevent proton decay. They should couple chirally to either left or right handed quarks but not to both, and mainly diagonally, i.e., they should couple to a single leptonic generation and to a single quark generation.

The effects of the experimental resolution were studied by passing both the signal and the background Monte Carlo (MC) events through the full DELPHI simulation and reconstruction chain.

Bhabha events, $e^+e^- \to \tau^+\tau^-$, $e^+e^- \to Z\gamma$, $e^+e^- \to WW$, $e^+e^- \to We\nu$, $e^+e^- \to ZZ$, and $e^+e^- \to Zee$ events were simulated with PYTHIA. In all four fermion channels, studies with the EXCALIBUR generator [5] were also performed. The two-photon ("$\gamma\gamma$") physics events were simulated using the TWOGAM [6] generator for quark channels.

A detailed description of the DELPHI detector and its performance, of the triggering conditions and of the readout chain can be found in reference [7].

2 Leptoquark Production Cross Sections

The most general Lagrangian which describes the leptoquark couplings belongs to a wide class of models [8] and can be described by

$$\mathcal{L} = \mathcal{L}_{F=2} + \mathcal{L}_{F=0} \tag{1}$$

$$\begin{aligned}\mathcal{L}_{F=2} &= (g_{1L}\bar{q}_L^c i\tau_2 l_L + g_{1R}\bar{u}_R^c e_R)S_1 + \tilde{g}_{1R}\bar{d}_R^c e_R \tilde{S}_1 \\ &+ g_{3L}\bar{q}_L^c i\tau_2 \overrightarrow{\tau} l_L \overrightarrow{S}_3 + (g_{2L}\bar{d}_R^c \gamma^\mu l_L + g_{2R}\bar{q}_L^c \gamma^\mu e_R)V_{2\mu} \\ &+ \tilde{g}_{2L}\bar{u}_R^c \gamma^\mu l_L \tilde{V}_{2\mu} + c.c.\end{aligned} \tag{2}$$

$$\begin{aligned}\mathcal{L}_{F=0} &= (h_{2L}\bar{u}_R l_L + h_{2R}\bar{q}_L i\tau_2 e_R)R_2 + \tilde{h}_{2L}\bar{d}_R l_L \tilde{R}_2 \\ &+ (h_{1L}\bar{q}_L \gamma^\mu l_L + h_{1R}\bar{d}_R \gamma^\mu e_R)U_{1\mu} + \tilde{h}_{1R}\bar{u}_R \gamma^\mu e_R \tilde{U}_{1\mu} \\ &+ h_{3L}\bar{q}_L \overrightarrow{\tau} \gamma^\mu l_L \overrightarrow{U}_{3\mu} + c.c.\end{aligned} \tag{3}$$

The q_L, l_L are the left-handed quark and lepton doublets, and the e_R, d_R, u_R are the right-handed charged leptons, down and up quarks respectively. The subscript L and R of the coupling constants denote the lepton chirality and the indices of the leptoquarks give the dimension of their SU(2) representation. Colour, weak isospin and generation flavour indices have been suppressed. The leptoquarks S (i.e. $S_1, \tilde{S}_1, \overrightarrow{S}_3$) and V (i.e. $V_2, \tilde{V}_2$) have fermion number F=3B+L=-2 (B and L are the baryon and lepton numbers respectively). The leptoquarks R (i.e. $R_2, \tilde{R}_2$) and U (i.e. $U_1, \tilde{U}_1, \overrightarrow{U}_3$) have fermion number F=3B+L=0. Leptoquarks S and R are scalars and leptoquarks V and U are vectors. The quantum numbers of the leptoquarks can be seen in [8].

Every coupling in the above expression $g_{1L}, ..., h_{3L}$ can be replaced by a generic Yukawa coupling g [9] (also designed by some authors as λ) which is scaled down to electromagnetic strength by assuming that $g^2/(4\pi) = k\alpha_{em}$, where k is allowed to vary.

Single production of leptoquarks in e^+e^- collisions was discussed by several authors in the literature. The production cross-section was computed within two different approaches. The first one, hereafter designated as the direct mechanism, corresponds to the diagrams represented on figure 1 [9, 10, 11]. The second one, designated as the resolved photon mechanism, correspond to the diagram of figure 2 [12, 13, 14].

In fact, in the direct processes each diagram is evaluated as the convolution of the $e\gamma$ amplitude with the probability of emission of a hard photon by an initial electron (parametrized by the Weizacker-Williams distribution [15], $F_{\gamma/e}(x)$). In the resolved photon mechanism, the same factorization of the hard photon (assuming also the Weizacker-Williams distribution) is done but the quark and gluon content of the photon is explicitly used by means of a structure function. In this structure function in addition to the point like contribution ($\gamma \to q\bar{q}$) a vector meson dominance contribution (VDM) is included. The Glück Reya Vogt parameterization (GRV) [16] of the photon parton distribution was used. Since the photon has different up-quark and down-quark contents and the production cross section is proportional to $(1+q)^2$ (where q is the leptoquark charge), leptoquarks of charge $q = -1/3(-2/3)$ and $q = -5/3(-4/3)$ have similar production cross sections [17].

In figures 3 and 4 are represented the single leptoquark total production cross sections at $\sqrt{s} = 202$ GeV, in function of the leptoquark mass, for the different leptoquark charges respectively for the direct and resolved processes. The Yukawa coupling constant g associated to the eqS vertex can have different definition according to different authors. The Pakvasa g definition is used as the common base. As was discussed in [9] in order to make the distributions in the reference compatible with the ones in [10] it is required to

take k=2 in [9]. On the other hand, in order to make [13, 17] compatible with [10] it is required to take in [13, 17] k=0.5.

In figure 5 are represented the ratios between the cross sections for the direct processes and the resolved ones, for the single leptoquark production at $\sqrt{s} = 202$GeV (in function of the leptoquark mass, and for the different leptoquark charges). For low mass values the VDM is dominant but at higher masses all the ratios converges to a common value below 1.

3 Single Leptoquark Generation

The search for singly produced leptoquarks at LEP is performed within the two distinct frameworks discussed previously:

- For resolved photon processes (case 1) a modified version of the PYTHIA [18] generator is used to generate leptoquarks of different mass values in e^+e^- collisions;
- For the direct processes (case 2) the ERATO generator [19] is used.

3.1 Case 1: Resolved Processes Framework

In this framework the PYTHIA Monte Carlo program [18] was used to generate both scalar and vector leptoquarks (with a modified version). As discussed above, the photon is expected to interact through its hadronic content which is described by a quark and gluon structure function. The Dress and Grassie parametrization of the structure function was used [20]. The spectrum of photons was generated according to the Equivalent Photon Approximation [21] and the maximum kinematically allowed squared four-momentum transfer Q^2_{max} was set to $s/4$.

The total production cross section was taken from reference [13] (assuming $k = 0.5$) which uses for the photon energy distribution $F_{\gamma/e}$ the Weizacker-Williams approximation.

The approach used in [17] is independent of the leptoquark chirality (i.e., leptoquarks can couple to either right or left handed particles but not to both) and is almost insensitive to whether the leptoquark is scalar or vector. For the same leptoquark charge, the vector production cross section is the double of the scalar one.

The value of the cross section taken from [13] concerns only production of negatively charged leptoquarks. To take into account the production of leptoquarks and antileptoquarks, the output cross section was multiplied by a factor 2.

3.2 Case 2: The ERATO Framework

In this framework the ERATO Monte Carlo program [19] was used to generate first family scalar and vector leptoquarks of different masses and evaluate the corresponding cross-sections.

The strategy followed by ERATO is slightly different from that of PYTHIA [18]: in the generation of a specific leptoquark signal which results in a particular three particle final state (lqq or νqq) apart from the leptoquark signal itself, the generator takes also into account all the contributions from the known Standard Model processes which would contribute to the specific final state. The interference effects are also considered.

The decay widths of the leptoquarks are parametrized by [8, 19],

$$\Gamma_J = f_J \frac{M}{8\pi} \sum_{i=1}^{N_{ch}} g_i^2, \tag{4}$$

where $J = 0, 1$, $f_0 = 1/2$ and $f_1 = 1/3$, and $N_{ch} = 1, 2$ depending on the available channels.

The single leptoquark production, via photon t-channel exchanges, is computed either by using the energy spectrum of the photon $F_{\gamma/e}$ parametrized according to a Weizsacker-Williams distribution [15] or by using the leading logarithmic approximation [22].

The value of the cross section evaluated by ERATO concerns only production of negatively charged leptoquarks. To take into account the production of leptoquarks and antileptoquarks, the output ERATO cross section was multiplied by a factor 2.

ERATO has the possibility of distinguishing all the different types of scalar and vector leptoquarks by choosing the appropriate parameters. The final results can be presented in terms of these different particles.

3.3 Cross Section Comparisons

Tables 1 and 2 show the comparisons between the two different frameworks in function of the leptoquark mass, for scalar and vector leptoquarks respectively. The cross section values presented assume that:

- the same type of couplings are used (by taking $k = 0.5$ for [13] and $k = 1$ in [19]);
- if the leptoquark can decay through the charged and the neutral decay mode the total cross section is the sum of the two corresponding contributions;
- leptoquark and anti-leptoquark are produced;
- the center of mass energy is $\sqrt{s} = 202$ GeV/c^2.

The cross section values obtained within the two different frameworks (Case 1 and Case 2, see above) are very similar (except for some special cases) and show a dependence on the mass and charge of the leptoquark.

4 Data Analysis

The final state corresponding to the decay of singly produced high mass leptoquark is characterised by a high transverse momentum jet recoiling against a lepton (neutral or charged) and some low energetic activity in the forward region.

At the pre-selection stage the events were classified according to the number of jets and of isolated leptons and photons. Details on the pre-selection are given in reference [23]. Only small adjustments were made with respect to the previous analysis. The minimum required charged multiplicity was six and all particles (excluding the isolated charged lepton, if present) were also forced into one jet using the Durham jet algorithm [24]. The monojet had to have at least one charged particle.

The following criteria were then applied to the events (level 1):

$\sigma(J=0)$ (pb)	Charge	120GeV/c^2	140GeV/c^2	160GeV/c^2	180GeV/c^2	200GeV/c^2
Case 2 :						
S_{1L}	$\frac{1}{3}$	0.732	0.408	0.215	0.086	0.002
S_{1R}	$\frac{1}{3}$	0.732	0.408	0.216	0.087	0.002
$\tilde{S}_{1R}$	$\frac{4}{3}$	0.256	0.134	0.066	0.024	0.001
S_{3L}	$\frac{4}{3}$	0.518	0.268	0.132	0.049	0.001
S_{3L}	$\frac{1}{3}$	0.732	0.408	0.215	0.086	0.002
R_{2L}	$\frac{5}{3}$	0.896	0.482	0.246	0.094	0.002
R_{2R}	$\frac{5}{3}$	0.896	0.482	0.246	0.094	0.002
R_{2R}	$\frac{2}{3}$	0.173	0.096	0.051	0.021	0.001
$\tilde{R}_{2L}$	$\frac{2}{3}$	0.173	0.096	0.051	0.021	0.001
Case 1 :						
	$\frac{1}{3}(\frac{5}{3})$	0.846	0.439	0.214	0.080	0.003
	$\frac{2}{3}(\frac{4}{3})$	0.251	0.123	0.057	0.021	0.001

Table 1: Cross section comparisons between ERATO generator and resolved photon processes only, for scalar leptoquark production at LEP for $\sqrt{s} = 202$ GeV.

- the total visible energy was required to be larger than $0.2\sqrt{s}$;
- no isolated photons were allowed in the event;
- the momentum of the monojet was required to be larger than 50 GeV/c and the sum of its electromagnetic and hadronic energy had to be greater than 30 GeV;
- for the leptoquark charged decay mode, one and only one isolated charged lepton was required. The charged lepton had to have hits on the vertex detector (VD), a momentum greater than 50 GeV/c and the ratio of its electromagnetic associated energy over the total (electromagnetic and hadronic) associated energy had to be higher than 0.1.

After this selection, more specific criteria were applied (level 2):

- Events should have a clear monojet topology. This cut was implemented requiring the Durham resolution variable in the transition from two to one jet (y_{cut}), to have a $-log_{10}(y_{cut})$ higher than 1.1.
- The monojet polar angle had to be between 30° and 150°.
- The ratio between the monojet electromagnetic energy and its total energy had to be smaller than 0.95. This cut reduce the contamination from Bhabha events.

In order to further reduce background contamination, mostly coming from $q\bar{q}$ and WW events, additional criteria were applied depending on the final channel (level 3):

$\sigma(J=1)$	$Charge$	$120 GeV/c^2$	$140 GeV/c^2$	$160 GeV/c^2$	$180 GeV/c^2$	$200 GeV/c^2$
Case 2 :						
V_{2L}	$\frac{4}{3}$	0.520	0.276	0.131	0.048	0.001
V_{2R}	$\frac{4}{3}$	0.520	0.276	0.131	0.048	0.001
V_{2R}	$\frac{1}{3}$	1.658	0.904	0.478	0.183	0.004
$\tilde{V}_{2L}$	$\frac{1}{3}$	1.658	0.904	0.478	0.183	0.004
U_{1L}	$\frac{2}{3}$	0.412	0.225	0.116	0.045	0.001
U_{1R}	$\frac{2}{3}$	0.398	0.222	0.115	0.045	0.001
$\tilde{U}_{1R}$	$\frac{5}{3}$	1.878	0.986	0.502	0.189	0.004
U_{3L}	$\frac{5}{3}$	3.820	2.020	1.012	0.378	0.009
U_{3L}	$\frac{2}{3}$	0.412	0.225	0.116	0.045	0.001
Case 1 :						
	$\frac{1}{3}(\frac{5}{3})$	1.692	0.878	0.427	0.161	0.006
	$\frac{2}{3}(\frac{4}{3})$	0.502	0.245	0.114	0.042	0.002

Table 2: Cross section comparisons between ERATO generator and resolved photon processes only, for vector leptoquark production at LEP for $\sqrt{s} = 202$ GeV.

- All particles were forced into two jets and the momentum of the second jet (in GeV/c) had to be smaller than $0.001 * (\theta_{j1-j2} - 180.)^2 + 15$, where θ is measured in degrees.

- For the leptoquark charged decay mode leptons were identified as electrons if there were no associated hits in the muon chambers, if the electromagnetic energy to the momentum ratio (E/P) was larger than 0.2 and if the lepton electromagnetic energy normalized to its total energy was larger than 0.9. It was required that:

  (i) The lepton was identified as an electron and its polar angle had to be between 30° and 150°;

  (ii) the angle between the electron and the monojet had to be larger than 100°.

  (iii) the number of charged tracks in the hemisphere opposed to the monojet direction was required to be less than 10;

- For the leptoquark neutral decay mode, where the contamination of $q\bar{q}$ is higher, the invariant mass of the two jets had to be smaller than 40 GeV/c^2.

In tables 3 and 4 the number of events which passed the different levels of selection are shown, together with the expected SM background for the charged and the neutral decay modes respectively.

Figure 6 show (at level 1), as an example, the lepton and jet momenta, and the angle between the lepton and the jet, for the leptoquark charged decay mode at a centre-of-mass energy of 202 GeV . Figure 7 show, at the same $\sqrt{s}$ and at level 1, the jet momentum and polar angle together with the SM expectation for the neutral decay mode.

A good agreement is observed between data and SM expectations both for the charged and neutral decay modes.

$\sqrt{s}$(GeV)	selection level					
	1		2		3	
192	20	(24.3±1.1)	10	(17.3±0.9)	0	(0.6±0.2)
196	76	(70.8±3.1)	54	(50.3±2.5)	3	(1.7±0.6)
200	91	(92.6±3.7)	57	(64.5±3.7)	3	(2.3±0.7)
202	57	(45.0±1.8)	38	(31.1±3.7)	0	(1.1±0.4)

Table 3: Number of events passing the sets of cuts corresponding to the selection levels described in the text for the charged decay mode.

$\sqrt{s}$(GeV)	selection level					
	1		2		3	
192	620	(661.0± 8.2)	42	(48.7±1.9)	1	(0.4±0.1)
196	1994	(1950.9± 24.2)	189	(143.0±5.8)	2	(1.2±0.3)
200	2167	(2074.5±26.8)	180	(168.9±6.7)	1	(1.7±0.5)
202	1062	(1002.1±12.9)	88	(81.5±3.2)	1	(0.8±0.2)

Table 4: Number of events passing the sets of cuts corresponding to the selection levels described in the text for the neutral decay mode.

In the charged decay mode 6 events passed all cuts in the data and the expected SM background was 5.7 ± 1.0. The jet-lepton invariant masses, calculated using the lepton energy, are for these events 114 GeV/c^2, 132 GeV/c^2, 141 GeV/c^2, 166 GeV/c^2 180 GeV/c^2 and 200 GeV/c^2.

In the neutral decay mode 5 events survived all cuts while the expected SM background was 4.1 ± 0.6. The invariant masses, calculated using the monojet transverse momentum, are 99 GeV/c^2, 108 GeV/c^2, 109 GeV/c^2, 113 GeV/c^2 and 121 GeV/c^2.

5 Results for Leptoquarks

Experimentally the existence of leptoquarks is constrained indirectly by low-energy data [25] and precision measurements of the Z^0 widths [26], and by direct searches at high energies [27, 28, 29, 30]. At the Tevatron the mass of scalar leptoquarks decaying to electron jet pairs was constrained to be above 225 GeV/c^2. At HERA, using the e^-p data, limits on leptoquark masses and couplings were set at $M_{LQ} > 216 - 275$ GeV/c^2. Using the e^+p data an excess of events was found in the data. The H1 collaboration measured a jet-lepton invariant mass of these events ranging from 187.5 GeV/c^2 up to

212.5 GeV/c^2. Rare processes, which are forbidden in the SM, also provide strong bounds on the λ/m_{LQ} ratio [31], where λ is the leptoquark-fermion Yukawa type coupling and m_{LQ} is the leptoquark mass.

	PYTHIA		ERATO	
mass(GeV/c^2)	Scalar	Vector	Scalar	Vector
120	14.4 ($\pm$1.7)	15.6 ($\pm$1.8)	15.7 ($\pm$1.9)	10.2 ($\pm$1.4)
140	24.4 ($\pm$2.2)	21.4 ($\pm$2.1)	24.9 ($\pm$2.5)	20.4 ($\pm$2.1)
160	32.8 ($\pm$2.3)	24.8 ($\pm$2.2)	33.2 ($\pm$2.9)	28.2 ($\pm$2.4)
180	30.8 ($\pm$2.5)	29.6 ($\pm$2.4)	34.0 ($\pm$2.5)	32.1 ($\pm$2.5)
200	37.6 ($\pm$2.7)	31.6 ($\pm$2.5)	36.0 ($\pm$2.7)	28.7 ($\pm$2.4)

Table 5: Efficiency for the charged decay mode.

For the charged decay mode, the detector efficiency as a function of the leptoquark mass are shown in table 5 both for PYTHIA and ERATO. Within the statistical errors the efficiencies are comparable for the two generators. The mass resolution at 160 GeV/c^2 is around 18 GeV/c^2.

	PYTHIA	ERATO	
mass(GeV/c^2)	Scalar	Scalar	Vector
120	16.8 ($\pm$1.8)	15.0 ($\pm$1.7)	14.6 ($\pm$1.7)
140	20.6 ($\pm$2.0)	18.8 ($\pm$1.9)	22.2 ($\pm$2.1)
160	25.2 ($\pm$2.2)	22.2 ($\pm$2.1)	24.6 ($\pm$2.2)
180	32.0 ($\pm$2.5)	27.8 ($\pm$2.4)	28.0 ($\pm$2.4)
200	36.5 ($\pm$3.0)	34.2 ($\pm$2.6)	29.4 ($\pm$2.4)

Table 6: Efficiency for the neutral decay mode.

For the neutral decay mode, the detector efficiency as a function of the leptoquark mass are shown in table 6 both for PYTHIA and ERATO. Within the statistical errors the efficiencies are comparable for the two generators. The mass resolution at 160 GeV/c^2 is around 30 GeV/c^2.

From the obtained invariant mass distributions, it is possible to set limits on the leptoquark coupling parameter λ. For $\beta = 1$ the invariant mass plot for the charged decay mode was used to set the limits. For $\beta = 0.5$ the invariant mass plots of the charged and the neutral decay modes were combined to set the limits.

The results of this analysis are used to set limits in the framework of reference [13], combining with data taken at a centre-of-mass energy of 189 GeV [33]. They are compared with those obtained using the ERATO generator (section 5.2).

5.1 Case 1: Resolved Processes Framework

Within this framework the coupling definitions used are the ones of [13] (λ=$\sqrt{4\pi k\alpha_{em}}$ with k=0.5). These limits, as a function of the leptoquark mass, are shown in figure 8 for both scalar and vector leptoquarks of different types and for the different charged decay branching ratios ($\beta = 1$ or $\beta = 0.5$).

The lower limits at 95% confidence level on the mass of a first generation leptoquark for a coupling parameter $\lambda = \sqrt{4\pi\alpha_{em}}$ are given in table 7, where different leptoquark types and branching ratios are considered [32].

	$\|Q\|$=1/3,5/3		$\|Q\|$=2/3,4/3	
	$\beta = 0.5$	$\beta = 1.0$	$\beta = 0.5$	$\beta = 1.0$
scalar	180.	180.	-	155.
vector	-	185.	169.	168.

Table 7: Lower limits (in GeV/c^2) at 95% confidence level on the the mass of a first generation leptoquark for a coupling parameter of λ=$\sqrt{4\pi k\alpha_{em}}$ within reference [13] frame work (k=0.5).

5.2 Case 2: ERATO framework

Within this framework the coupling definitions are different from the ones of [13] (see the introduction). The obtained limits, as a function of the leptoquark mass, are shown in figure 9 for both scalar and vector leptoquarks of different types and for the different charged decay branching ratios ($\beta = 1$ or $\beta = 0.5$).

The lower limits at 95% confidence level on the mass of a first generation leptoquark are given in table 8, where different leptoquark types and branching ratios are considered [32].

Leptoquark	*Charge*	*B*	*Type*	*Mass Limit* (GeV/c^2)
S_{1L}	$\frac{1}{3}$	0.5	scalar	180.
S_{1R}	$\frac{1}{3}$	1.0	scalar	180.
$\tilde{S}_{1R}$	$\frac{4}{3}$	1.0	scalar	158.
U_{1L}	$\frac{2}{3}$	0.5	vector	171.
U_{1R}	$\frac{2}{3}$	1.0	vector	170.
V_{2R}	$\frac{1}{3}$	1.0	vector	188.

Table 8: Lower limits (in GeV/c^2) at 95% confidence level on the the mass of a first generation leptoquark for a coupling parameter of λ=$\sqrt{4\pi k\alpha_{em}}$ (with k=1.0 within the ERATO framework).

6 Summary

A search for first generation leptoquarks was performed using the data collected by the DELPHI detector at $\sqrt{s}$ =192-202 GeV. Both neutral and charged decay modes of scalar and vector leptoquarks were searched for. No evidence for a signal was found in data. Limits on leptoquark masses were set at 95% confidence level (see table 7 for results). Consistency with a second theoretical framework has been checked (table 8).

Acknowledgements

We would like to thank M. Doncheski and A.Djouadi for the very useful discussions on the leptoquark production. We are greatly indebted to our technical collaborators and to the funding agencies for their support in building and operating the DELPHI detector. Very special thanks are due to the members of the CERN-SL Division for the excellent performance of the LEP collider.

References

[1] DELPHI Coll., P. Abreu et al., Phys.Lett. **B446** (1999) 62.

[2] P. Langacker, Phys. Rep. **72** (1981) 185.

[3] See for example S. Dimopoulos, Nucl. Phys. **B168** (1981) 69.

[4] See for example B. Schremp and F. Schremp, Phys. Lett. **153B** (1985) 101.

[5] F.A. Berends, R. Pittau, R. Kleiss, Comp. Phys. Comm. **85** (1995) 437.

[6] S. Nova, A. Olchevski and T. Todorov, "TWOGAM, a Monte Carlo event generator for two photon physics", DELPHI Note 90-35 PROG 152.

[7] DELPHI coll., P. Aarnio et al., NIM **A303** (1991) 233;
DELPHI Coll., P. Abreu et al., Nucl. Instr. Methods **A378** (1996) 57.

[8] W. Buchmuller, R.Ruckl, D.Wyler, Phys. Lett. **B191** (1987) 442;

[9] H.Nadeau, D.London, Phys. Rev D **47** (1993) 3742.

[10] J.L.Hewett, S.Pakvasa, Phys. Lett. **B227** (1989) 178.

[11] H.Nadeau, D.London, G.Bélanger, UdeM-LPN-TH-93-160, McGill-93/29, hep-ph/9309243, September 1993.

[12] O.J.P.Eboli, E.M.Gregores, M.B.Magro, P.G.Mercadante, S.F.Novaes, Phys. Lett. **B311** (1993) 147-152.

[13] M. Doncheski and S. Godfrey, Phys. Rev. **D49** (1994) 6220.

[14] A.Djouadi, J.Ng, T.G.Rizzo, SLAC-PUB-95-6772, GPP-UdeM-TH-95-17, TRI-PP-95-05, June 1995.

[15] C.F.von Weizsacker, Z.Phys. **88** (1934) 612; E.J.Williams, Phys. Rev. **45** (1934) 729; M.Chen, P.Zerwas, Phys.Rev.**D12** (1975) 187.

[16] M. Gluck et al., Phys. Rev. **D46** (1992) 1973 and Phys. Rev. **D45** (1992) 3986.

[17] M. Doncheski and S. Godfrey, Phys. Lett. **B393** (1997) 355.

[18] T. Sjöstrand, Comp. Phys. Comm. **82** (1994) 74;
T. Sjöstrand, Pythia 5.7 and Jetset 7.4, CERN-TH/7112-93.

[19] C.G.Papadopoulos, DEMO-HEP-97/04, hep-ph/9703372, March 1997.

[20] M.Dress, K.Grassie, Z.Phys.**C28** (1985) 451-462.

[21] P.Aurenche, G.A.Schuller (conveners), $\gamma\gamma$ Physics, in "Physics at LEP2", CERN 96-01, eds G.Altarelli, T.Sjostrand and F.Zwirner, Vol.1 (1996) 291.

[22] F.A.Berends, R.Pittau, R.Kleiss, Nucl.Phys. bf B424 (1994) 308.

[23] DELPHI Coll., P. Abreu et al., Phys. Lett. **B393** (1997) 245. DELPHI Coll., P. Abreu et al., CERN/EP98-169, accepted by E. Phys. J. C.

[24] S. Catani et al., Phys. Lett. **B269** (1991) 432.

[25] O. Shanker, Nucl. Phys. **B204** (1982) 375; W. Buchmuller and D.Wyler, Phys. Lett. **B177** (1986) 377; J.L. Hewett and T.G. Rizzo, Phys. Rev. **D36** (1987) 3367; M. Leurer, Phys. Rev. **D49** (1994) 333 and Phys. Rev. **D50** (1994) 536.

[26] J.K. Mizukoshi, O.J.P. Eboli and M.C. Gonzalez-Garcia, CERN-TH 7508/94 (1994); G. Bhattacharya, J. Ellis and K. Sridhar, CERN-TH 7280/94 (1994).

[27] CDF Coll., F. Abe et al., hep-ex/9708017; D0 Coll., B. Abbott et al., Fermilab-Pub-97/252-E (hep-ex/9707033).

[28] ZEUS Coll., M. Derrick et al., Phys. Lett. **B306**, 1993 (173); H1 Coll., I. Abt et al., Nucl. Phys. **396**, (1993) 3.

[29] H1 Coll., C. Adloff et al., DESY 97-024 (hep-ex/9702012); ZEUS Coll., J. Breitweg et al. DESY 97-025 (hep-ph/9702015); updated analysis see B. Straub, talk presented at LP'97 Symposium, Hamburg, July 1997.

[30] ALEPH Coll., D. Decamp et al., CERN PPE/91-149. DELPHI Coll., P. Abreu et al., Phys. Lett. **B316** (1993) 620; L3 Coll., B. Adeva et al., Phys. Lett. **B261** (1991) 169; OPAL Coll., G. Alexander et al., Phys. Lett. **B263** (1991) 123;

[31] S. Davidson et al., Z. Phys. **C61** (1994) 613.

[32] J.L. Hewett and T.G. Rizzo, hep-ph/9703337.

[33] DELPHI99-80 CONF 267, 15 June 1999.

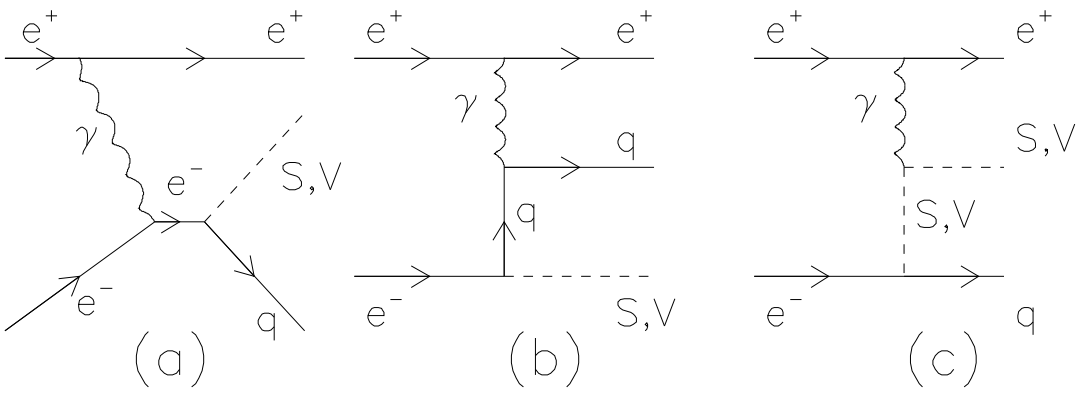

Figure 1: The direct contribution for single leptoquark production in e^+e^- collisions.

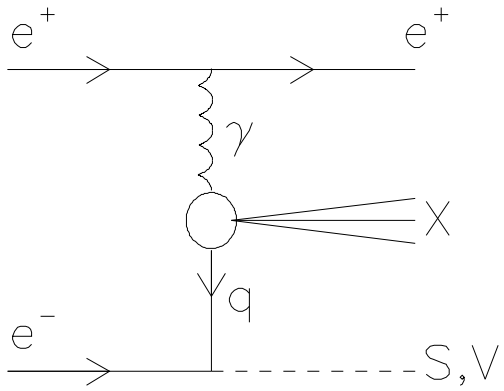

Figure 2: The resolved photon contribution for single leptoquark production in $e\gamma$ (a) and e^+e^- (b) collisions.

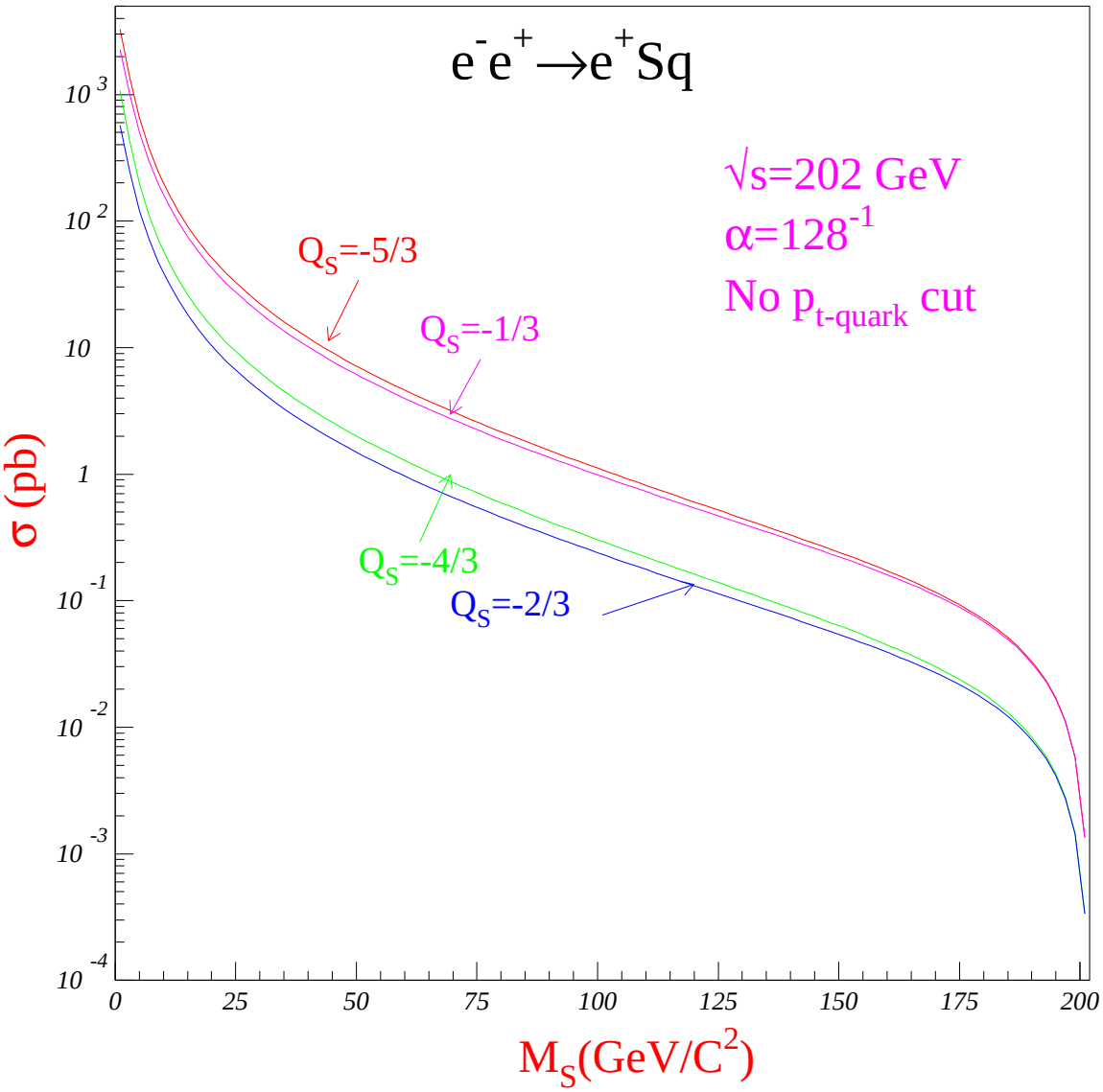

Figure 3: Single leptoquark production cross section in e^+e^- collisions for different leptoquark charges in function of the leptoquark mass for the direct processes.

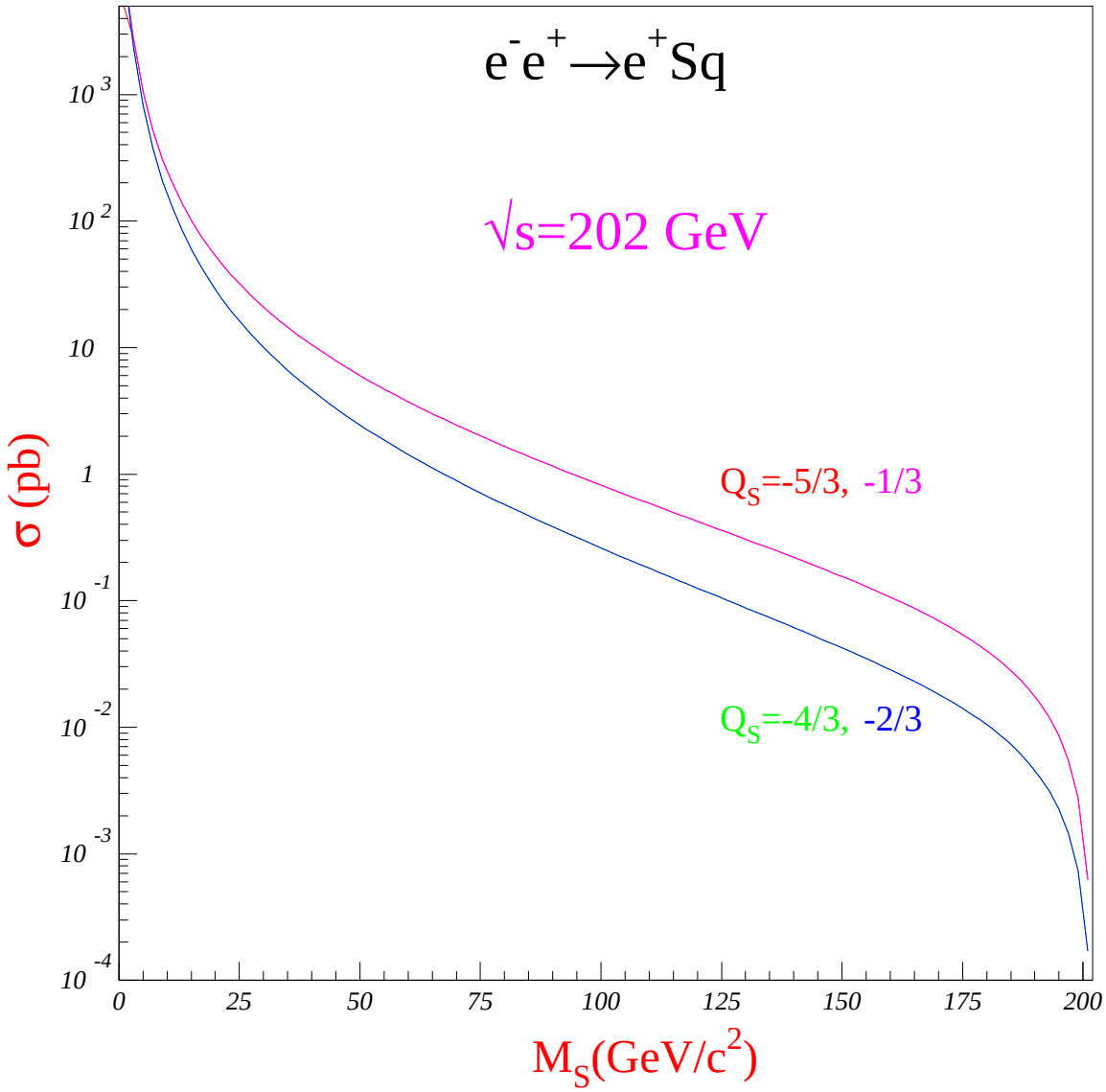

Figure 4: Single leptoquark production cross section in e^+e^- collisions for different leptoquark charges in function of the leptoquark mass for the resolved processes.

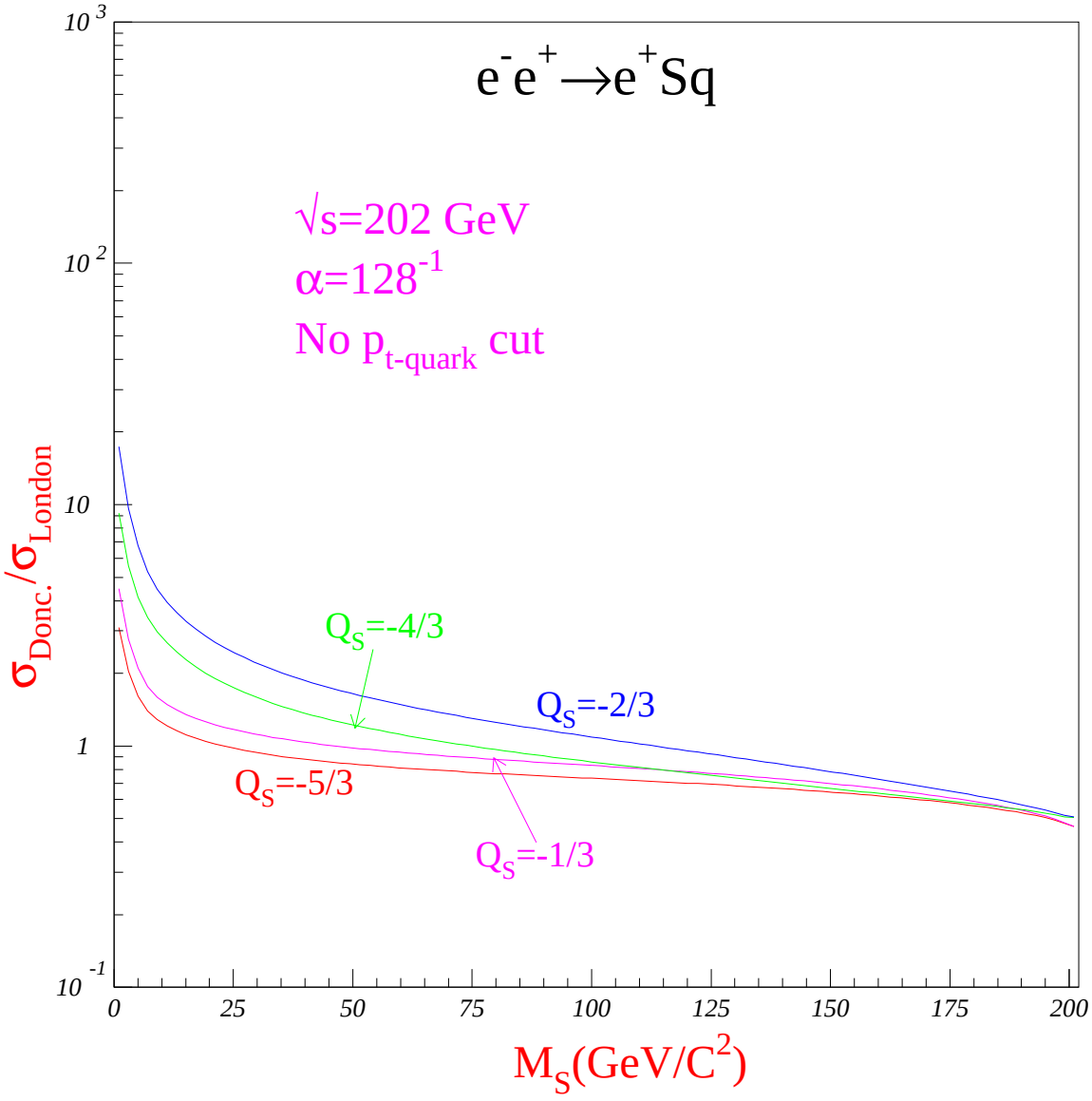

Figure 5: Ratio (between resolved and direct processes) of single leptoquark production cross sections in e^+e^- collisions for different leptoquark charges in function of the leptoquark mass.

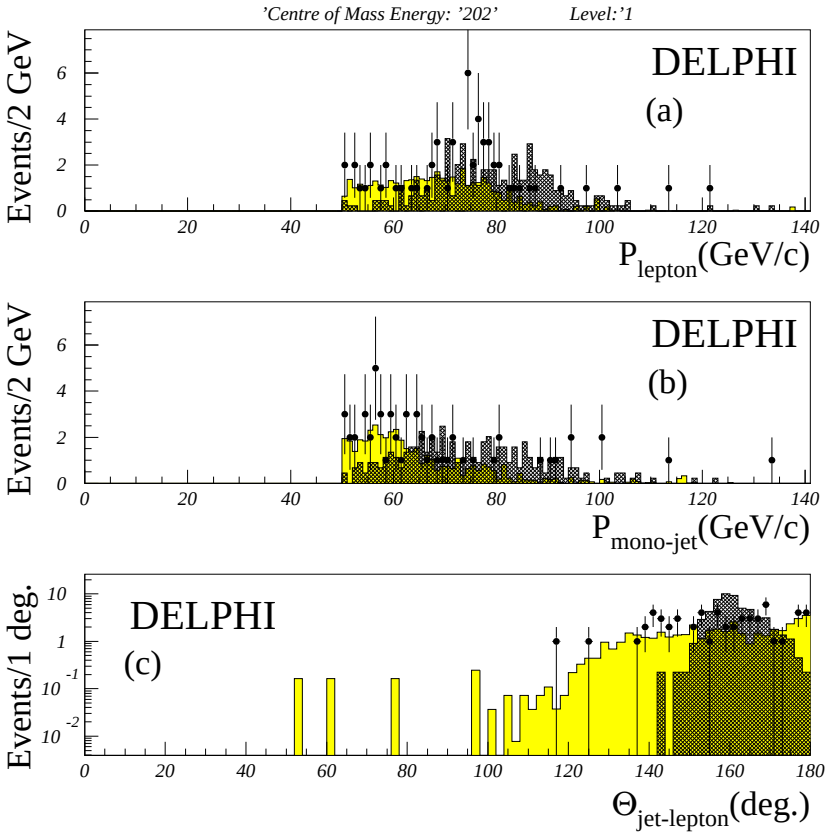

Figure 6: Leptoquark search: the electron momentum (a), the charged jet momentum (b) and the angle between the jet and electron momenta (c). The dots show the data, the light shaded region shows the SM simulation and the dark shaded region a signal simulation with arbitrary normalization.

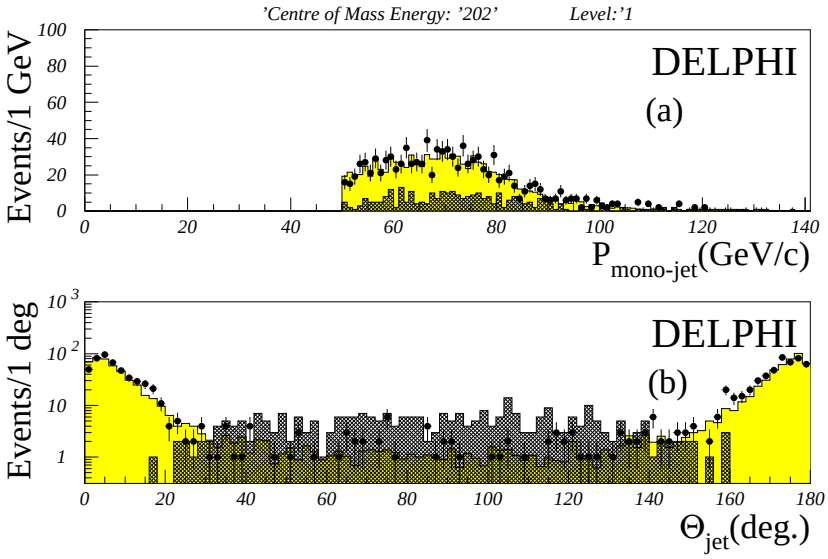

Figure 7: Leptoquark search: the electron momentum (a), the charged jet momentum (b) and the angle between the jet and electron momenta (c). The dots show the data, the light shaded region shows the SM simulation and the dark shaded region a signal simulation with arbitrary normalization.

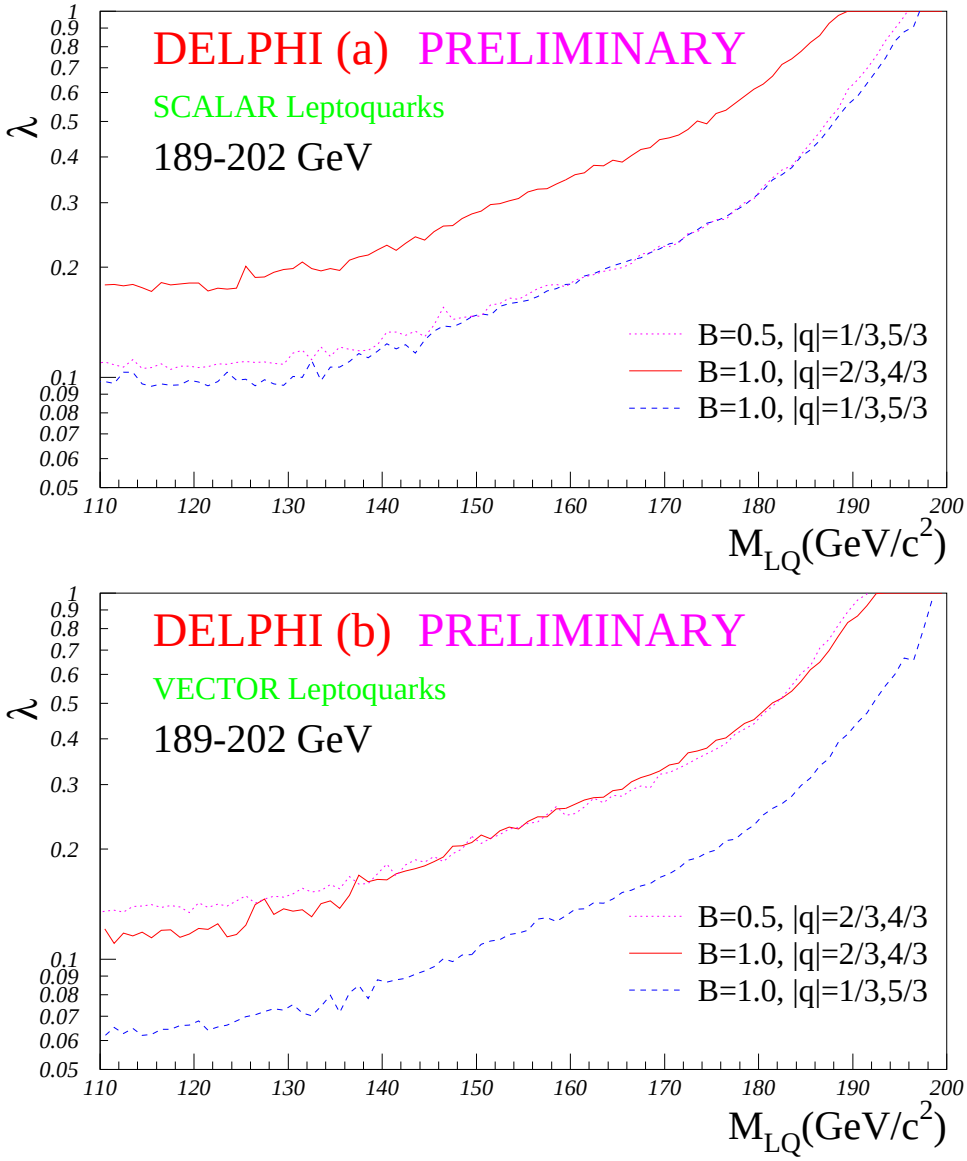

Figure 8: 95% confidence level limits on the coupling λ as a function of the leptoquark mass for scalar (and) and vector (botom) leptoquarks within the Doncheski framework.

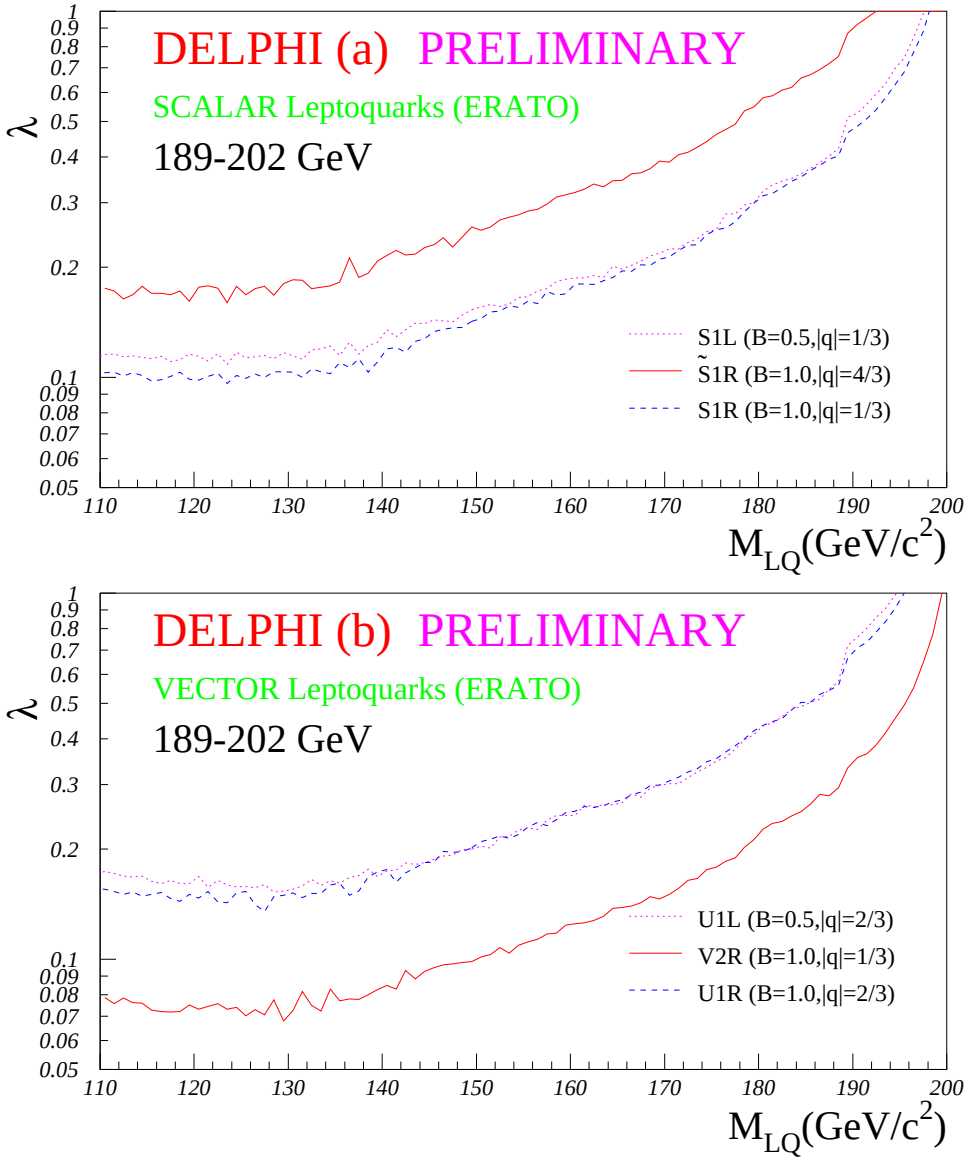

Figure 9: 95% confidence level limits on the coupling λ as a function of the leptoquark mass for scalar (top) and vector (botom) leptoquarks within the ERATO framework.